Low-Loss and High-Voltage III-Nitride Transistors for Power Switching Applications

Masaaki Kuzuhara, *Fellow, IEEE*, and Hirokuni Tokuda

(Invited Paper)

***Abstract*— This paper describes recent technological advances on III-nitride-based transistors for power switching applications. Focuses are placed on the progress toward enhancing the breakdown voltage, lowering the ON-resistance, suppressing current collapse, and reducing the leakage current in AlGaN/GaN high-electron mobility transistors (HEMTs). Recent publications revealed that the tradeoff relation between ON-resistance and breakdown voltage in AlGaN/GaN HEMTs exceeded the SiC limit and was getting close to the GaN limit; however, the breakdown voltage achieved was still lower than the theoretical impact ionization limit. A novel process featuring strain-controlled annealing with a metal stack, including Al gave rise to significant reduction in the sheet resistance in AlGaN/GaN heterostructures, suggesting the possibility of dramatic reduction in ON-resistance of GaN-based power devices. Some of the interesting approaches to suppress current collapse indicated that surface trapping effects must be controlled by the optimization of surface processing as well as by the reduction of bulk traps in the epitaxial layers. Close correlation between the local gate leakage current and point defects exposed on the free-standing GaN substrate demonstrated that further reduction of defects on bulk GaN substrates is truly required as future challenges.**

***Index Terms*— Breakdown voltage, current collapse, field plate (FP), GaN, gate leakage, high-electron mobility transistor (HEMT), ON-resistance.**

I. Introduction

III-NITRIDE-BASED transistors represented by AlGaN/GaN high-electron mobility transistors (HEMTs) are promising as low-loss and high-voltage switching devices to be utilized for a variety of power conversion circuits. Since GaN is a material having a wide bandgap of 3.4 eV with a direct transition band structure, it inherently shows a high critical electric field, low intrinsic carrier concentration, high-electron mobility, and high-drift velocity. In addition, capability of growing high-quality heterojunctions, such as AlGaN/GaN and InAlN/GaN, has enabled us to achieve high-density 2-D electron gas (2-DEG) of $>10^{13}$ cm^{-2} with a high-electron mobility of exceeding 2000 $cm^2/V\,s$.

Manuscript received July 9, 2014; revised September 5, 2014; accepted September 8, 2014. Date of publication November 26, 2014; date of current version January 20, 2015. This work was supported by a Grant-in-Aid of Basic Research (C) under Grant 25420328 and Grant 24560399 through the Ministry of Education, Culture, Sports, Science, and Technology, Japan. The review of this paper was arranged by Editor M. Bakowski.

The authors are with the Department of Electrical and Electronics Engineering, University of Fukui, Fukui 910-8507, Japan (e-mail: kuzuhara@fuee.u-fukui.ac.jp; htokuda@u-fukui.ac.jp).

Color versions of one or more of the figures in this paper are available online at http://ieeexplore.ieee.org.

Digital Object Identifier 10.1109/TED.2014.2359055

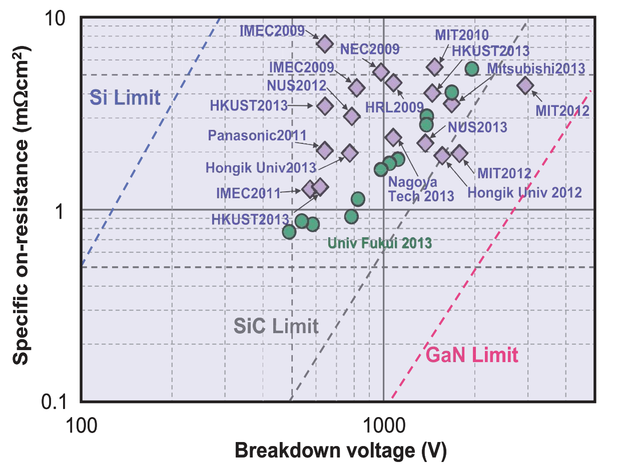

Fig. 1. Present status of specific ON-resistance versus breakdown voltage. Referred data can be found in [1]–[18].

Great efforts have been made over the last decade to improve the tradeoff relationship between breakdown voltage and specific ON-resistance of nitride-based transistors. In AlGaN/GaN HEMTs, the progress has been achieved by optimizing the device geometry, reducing the defect density in the epitaxial layers, improving the quality of buffer layers, and introducing newly developed process technologies. Fig. 1 shows reported values of specific ON-resistance as a function of breakdown voltage for GaN-based HEMTs, including our developed AlGaN/GaN HEMTs with varied gate-to-drain spacing [1]–[18]. It is evident that the power switching capability of AlGaN/GaN HEMTs is already far beyond the Si limit, partly exceeds the SiC limit, and is getting close to the GaN limit.

In this paper, technological advances on AlGaN/GaN HEMTs have been described, including our recent results for improving dc and pulsed performance of AlGaN/GaN HEMTs. Focuses are placed on the progress toward enhancing the breakdown voltage, lowering the ON-resistance, suppressing current collapse, and reducing the leakage current by introducing free-standing GaN substrates. Section II discusses experimental and simulated results performed to increase breakdown voltages of AlGaN/GaN HEMTs. Section III presents several technologies to reduce the ON-resistance of AlGaN/GaN HEMTs by lowering contact resistances and access resistances. In Section IV, experimental attempts are presented for the suppression of current collapse. Section V reports the advantage of using free-standing GaN substrate to reduce gate leakage current in AlGaN/GaN HEMTs. Finally, the conclusion is drawn in Section VI.

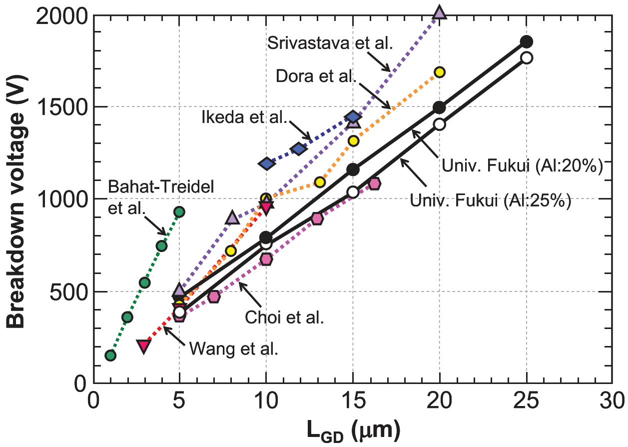

Fig. 2. Breakdown voltage plotted as a function of gate-to-drain distance. Referred data can be found in [19]–[24].

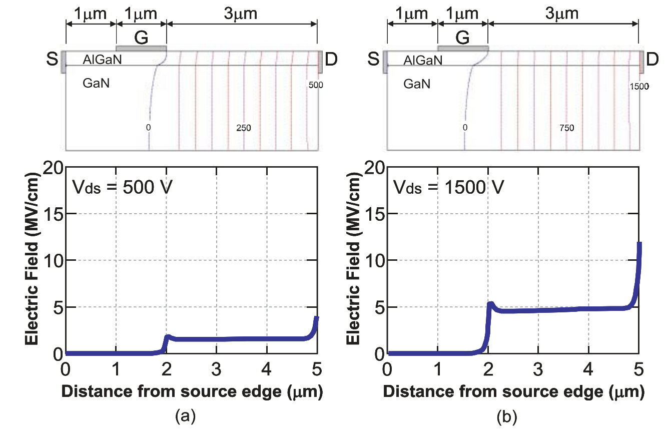

Fig. 3. Simulated electric field distribution between gate and drain in AlGaN/GaN HEMT at drain voltage of (a) 500 and (b) 1500 V.

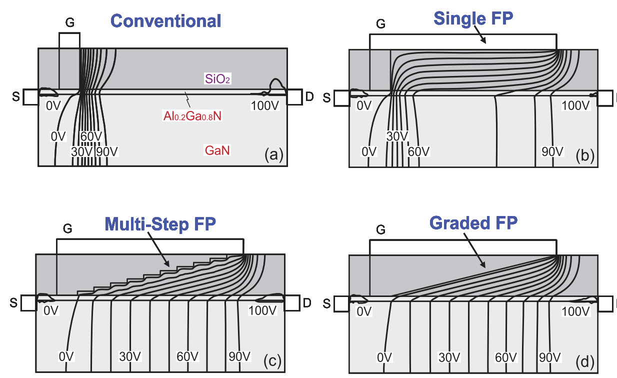

Fig. 4. Simulated equipotential contour lines in AlGaN/GaN HEMTs for (a) without FP, (b) single FP, (c) multistep FP, and (d) graded FP. The applied drain voltage is 100 V.

II. Breakdown Voltage

A large number of experimental results have been reported on the measured three-terminal breakdown voltage for AlGaN/GaN HEMTs. Fig. 2 shows examples of measured results plotted as a function of the distance between gate and drain (L_{gd}) for AlGaN/GaN HEMTs. The results indicate that the breakdown voltage is linearly proportional to L_{gd} in the breakdown voltage range up to at least 2000 V [19]–[24]. The averaged breakdown electric field ranges from 0.6 to 1.6 MV/cm [10]–[13], [25], which is still much lower than the expected impact ionization limit of 3 MV/cm. In general, the electric field concentrates at the gate edge in the drain side, as calculated by the 2-D computer simulation [26]. Such nonuniform electric field distribution does not guarantee the linear increase in the breakdown voltage, but is more likely to exhibit gradually saturated characteristics. Thus, the results shown in Fig. 2 imply that the lateral electric field along gate-to-drain direction is not concentrated at the gate edge, but more widely distributed or almost constant [27], [28].

Provided that magnitudes of positive and negative polarization charges (including spontaneous and piezoelectric charges), located at the interface and the surface of the AlGaN barrier layer, respectively, are mutually balanced, more uniform lateral electric field distributions could be accomplished along gate-to-drain. By applying strong drain voltages, 2-DEG charges in the channel are almost totally depleted, accompanied by the reduction in the ionized surface donor charge [29]. Hence, remaining charges between gate and drain would be a pair of balanced positive and negative polarization charges, resulting in constant electric field distribution, which is similar to the superjunction concept used in Si MOSFETs [30] and GaN-based diodes [31].

Fig. 3(a) and (b) shows the electric field distribution between gate and drain, based on 2-D computer simulation by assuming balanced polarization charges and depletion of 2-DEG charges. When positive and negative polarization charges are balanced, the electric field distribution in the channel becomes almost constant throughout the gate-to-drain region regardless of drain bias voltages assumed. However, since passivation films and/or GaN cap layer are formed in the actual AlGaN/GaN HEMTs, further study is needed whether the net surface negative charges balance with the positive polarization ones at the AlGaN/GaN interface. It is also an open question why the experimentally estimated lateral critical electric field is much lower than the theoretical limit. To solve such discrepancy, it would be of importance to investigate undesirable leakage current mechanisms related to the high density of crystal defects.

In addition, to make a gate-to-drain spacing longer, introducing field plate (FP) is also an effective way for increasing the breakdown voltage. The validity of FP has been recognized since early 2000s [32]–[34], and HEMTs with multi-FP were also reported [35], [36]. The simulation results on how the electric field distribution are modified by the number of FP steps are shown in Fig. 4(a)–(d), where equipotential contour lines are depicted. By increasing the number of step [Fig. 4(b) and (c)], the peak electric field along the gate-to-drain direction is decreased and the field distribution spreads, resulting in improved breakdown characteristics. The most suitable structure is the graded FP [Fig. 4(d)], although a special process is required for fabricating such a structure [19], [37].

It is known that AlGaN/GaN HEMTs tend to suffer from a high-gate leakage current originating from the leaky

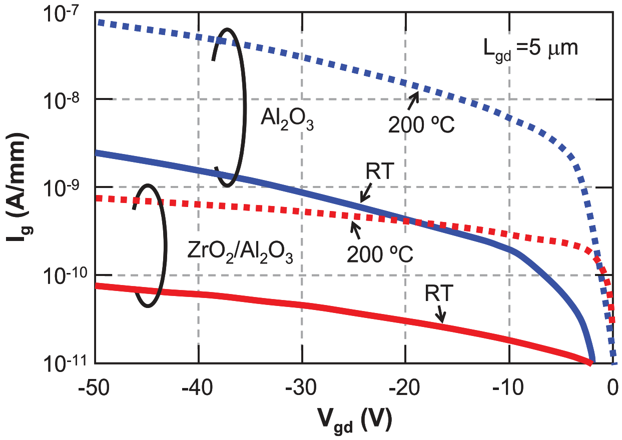

Fig. 5. Two-terminal reverse gate *I–V* characteristics of AlGaN/GaN MIS-HEMTs with gate insulator of composite ZrO_2/Al_2O_3 and single Al_2O_3 measured at room temperature and 200 °C.

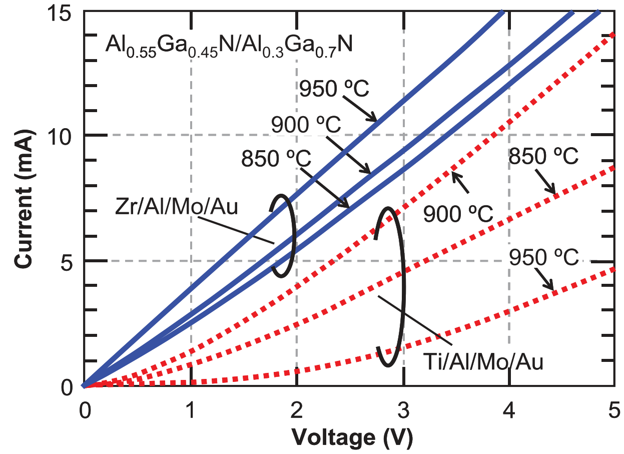

Fig. 6. *I–V* characteristics of $Al_{0.55}Ga_{0.45}N/Al_{0.3}Ga_{0.7}N$ HEMT with ohmic metals of Zr/Al/Mo/Au and Ti/Al/Mo/Au annealed at different temperatures.

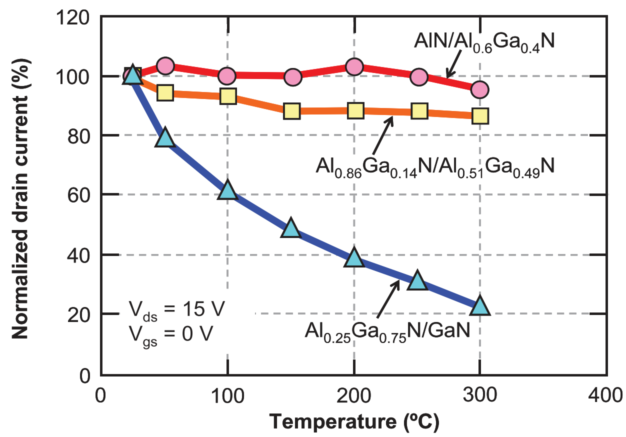

Fig. 7. Temperature dependences of drain current for AlGaN-channel HEMTs ($AlN/Al_{0.6}Ga_{0.4}N$ and $Al_{0.86}Ga_{0.14}N/Al_{0.51}Ga_{0.49}N$) and conventional AlGaN/GaN HEMT.

Schottky barrier at the metal–semiconductor interface. One of the effective ways to suppress such a high-gate leakage is the use of metal–insulator–semiconductor (MIS) structure for the gate. As a gate insulator, material properties of high resistivity, high-breakdown field, low-interface state density, and high permittivity are required. A large number of insulators, such as SiO_2, SiN, Al_2O_3, ZrO_2, HfO_2, and AlN, have been developed for fabricating MIS-HEMTs [38]–[43], and have been deposited with a variety of methods, including chemical vapor deposition (CVD), atomic layer deposition (ALD), sputtering, electron beam evaporation, and *in situ* SiN growth by metal—organic CVD [44]–[48]. Using ALD, we have developed a ZrO_2/Al_2O_3 double layered gate insulator with Al_2O_3 being the bottom and have shown that the composite insulator is advantageous in terms of low leakage current even at high temperatures. As shown in Fig. 5, a composite ZrO_2/Al_2O_3 insulator resulted in a reduced gate leakage current by two orders of magnitude at 200 °C, as compared with those with a single-layered insulator of ZrO_2 or Al_2O_3 [49].

III. ON-RESISTANCE

Lowering the ON-resistance is an important challenge for achieving high-efficiency operation in power switching circuits with AlGaN/GaN HEMTs. The ON-resistance between source and drain is expressed as the sum of contact resistance of source/drain electrodes, access resistance between source and gate, channel resistance beneath the channel, and access resistance between gate and drain.

Various kinds of metal stacks and corresponding annealing conditions have been attempted to obtain lower contact resistances in AlGaN/GaN HEMTs [50]–[54]. The commonly used metal stacks are Ti/Al/Ni/Au and Ti/Al/Mo/Au, and a contact resistance of 0.2–0.5 Ωmm has been typically reported. Gold-free ohmic metals have also been developed to ensure compatibility with the Si fabrication process [15], [55], [56]. Although good ohmic contact behaviors are obtained for an AlGaN barrier with relatively a low-Al composition of 0.15–0.3, it becomes rather difficult to obtain a reasonable contact resistance for AlGaN barriers with a high-Al composition of >0.5. For such HEMTs having a barrier layer with high-Al composition, Yafune *et al.* [57] have introduced a new metal stack of Zr/Al/Mo/Au and reported a relatively low value in contact resistance. Fig. 6 shows current–voltage ($I–V$) characteristics measured between ohmic metals on $Al_{0.55}Ga_{0.45}N/Al_{0.3}Ga_{0.7}N$ HEMTs, in which ohmic metal stacks composed of Zr/Al/Mo/Au and Ti/Al/Mo/Au were annealed at 850 °C, 900 °C, and 950 °C. Almost linear *I–V* characteristics were observed for Zr/Al/Mo/Au annealed at 950 °C, while only nonlinear characteristics were noticed for Ti/Al/Mo/Au. The reason for the better ohmic characteristics with Zr/Al/Mo/Au is that metals (presumably Zr and Al) in Zr/Al/Mo/Au penetrate more deeply into the $Al_{0.55}Ga_{0.45}N$ barrier layer than those in Ti/Al/Mo/Au, as reported in [57].

Two kinds of AlGaN-channel HEMTs, composed of $AlN/Al_{0.6}Ga_{0.4}N$ and $Al_{0.86}Ga_{0.14}/Al_{0.51}Ga_{0.49}N$, have been fabricated using Zr/Al/Mo/Au as ohmic electrodes [58], [59]. Fig. 7 shows the temperature dependence of drain current measured at temperatures up to 300 °C. The drain current was normalized with the values measured at room temperature. It is evident that the AlGaN-channel with a higher Al composition

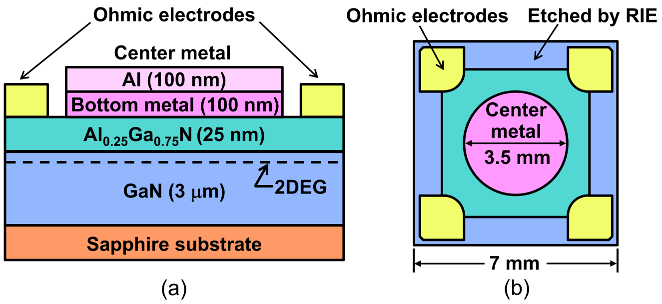

Fig. 8. (a) Cross-sectional and (b) top view of samples for measuring sheet electron density and mobility.

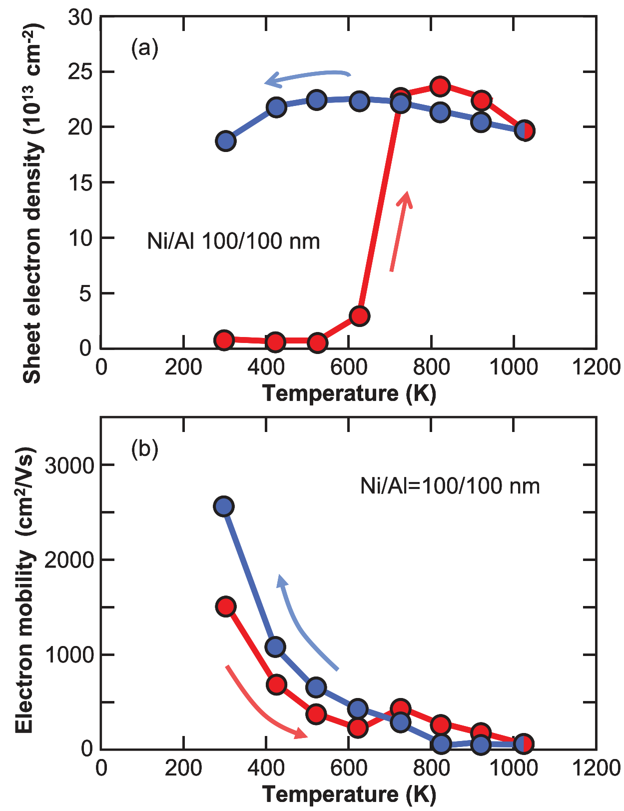

Fig. 9. Temperature dependences of (a) sheet electron density and (b) electron mobility of AlGaN/GaN heterostructure deposited with Ni/Al. Arrows indicate temperature change directions.

(>0.5) exhibits extremely stable drain current behaviors with respect to the device temperature up to 300 °C. Although further improvements, such as lowering the contact resistance are needed, the AlGaN-channel HEMT is promising in terms of stable operation at elevated temperatures with sufficiently high-breakdown voltages [14].

Access resistances of HEMTs are determined by the product of 2-DEG density (n_s) and electron mobility (μ). Since those values measured at room temperature in AlGaN/GaN heterostructures are typically in the range of 8–10 $\times$ 10^{12} cm^{-2} and 1500–2000 cm^2/V s, respectively, the corresponding sheet resistance turns out to be ~300–500 Ω/sq. If one could increase both n_s and μ, the sheet resistance would be significantly reduced, leading to extremely low-access resistance. Regarding the 2-DEG mobility at low temperatures, theoretical and experimental studies have been extensively made to understand the dominant transport mechanisms at the AlGaN/GaN interface. As a result, a mobility of 7500 cm^2/V s at 10 K was reported in [60], and it was increased year by year, reaching 167 000 cm^2/V s at 0.3 K in [61]. Meanwhile, the room temperature mobility in AlGaN/GaN heterostructure has not been increased over the last decade, even though significant progress has been achieved in epitaxial growth technologies. This is because, the room temperature electron mobility is mainly governed by polar-optical phonon scattering [62], [63], which is almost independent of the epitaxial layer quality. A room temperature electron mobility of 2019 cm^2/V s has been reported in [64], and it was increased to 2200 cm^2/V s in [65], corresponding to an increase by only 9%.

An interesting method to increase room temperature electron mobility is to introduce an additional tensile strain in an AlGaN layer. Azize and Palacios [66] reported a mobility increase by etching a Si substrate from the backside for controlling the tensile strain in AlGaN. Fehlberg *et al.* [67] reported a high mobility of 2380 cm^2/V s by depositing SiN films with varied deposition conditions, resulting in introduction of strain in an AlGaN layer. In addition, Im *et al.* [68] controlled the tensile strain by varying the buffer layer thickness and fabricated an AlGaN/GaN HEMT with increased n_s of 1×10^{14} cm^{-2}, though the mobility was low.

Our group have reported significant increases in both n_s and μ by annealing an AlGaN/GaN heterostructure in vacuum with deposited metals composed of Ti/Al or Ni/Al [69]–[71]. Fig. 8 shows cross-sectional and top views of the measured AlGaN/GaN sample with van der Pauw configuration. Ohmic electrodes were formed in the four corners and an additional metal consisting of double layered metal stack, center metal, was evaporated. The sample was set to the Hall measurement system and the temperature dependence of n_s and μ was measured with increasing and decreasing sample temperatures ranging from 300 (room temperature) to 1020 K. All the measurements were carried out in vacuum (~1×10^{-3} torr). An example of the measured temperature dependences in n_s and μ is shown in Fig. 9(a) and (b). With increasing temperature from 300 K, n_s showed a sudden increase at ~650 K and had a peak at 820 K followed by a slight decrease. By decreasing temperature from 1020 K, n_s was slightly increased and then decreased. Meanwhile, μ showed a hump at ~650 K with increasing temperature from 300 K. It is to be noted that both n_s and μ did not take the same paths in the cycle of heating and cooling, resulting in an increase in n_s by one order of magnitude and an increase in μ by 70% at room temperature. The amount of increased μ depended on the thickness of Ni/Al and a value of over 3000 cm^2/V s was achieved by optimizing the thickness [72].

The microstructure of the annealed metals with Ti/Al (Bottom: Ti, Top: Al) and with Al/Ti (Bottom: Al, Top: Ti) was investigated by Auger electron spectroscopy [70], where the increases in n_s and μ were only observed for Ti/Al and not for Al/Ti. The results indicate that the top Al layer diffuses into the bottom Ti layer for Ti/Al, whereas Ti does not diffuse into Al for Al/Ti, suggesting that the diffusion of top Al layer

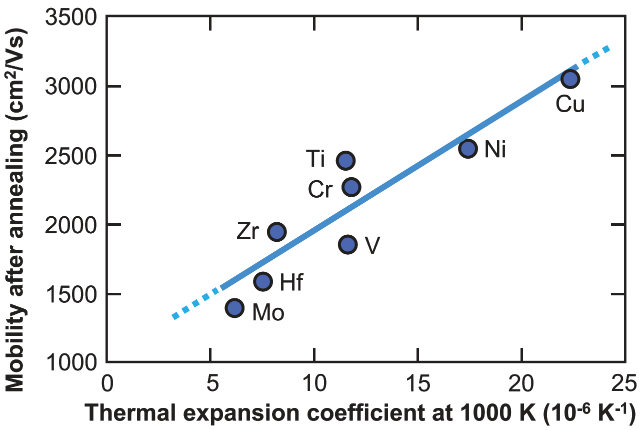

Fig. 10. Room temperature electron mobility of AlGaN/GaN heterostructures after annealing as a function of thermal expansion coefficient of the bottom metal.

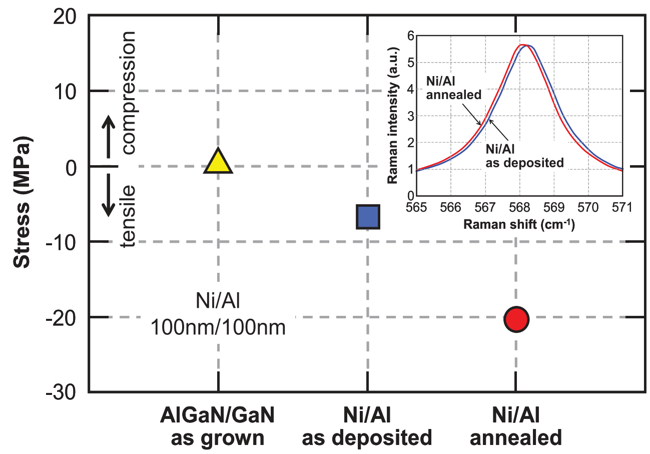

Fig. 11. Stress values measured by Raman spectroscopy for AlGaN/GaN bare surface, as-deposited Ni/Al (100/100 nm), and annealed Ni/Al (100/100 nm). Inset: Raman signal.

into the bottom metal plays a key role for the increases in n_s and μ. One might think that the measured n_s and μ did not correspond to those of 2-DEG, but those of center metal. However, such possibilities are excluded by the experimental results [69]–[71]. The increases in n_s and μ were not observed when the center metal was a monolayer of Ti or Al, and also the amount of increase in n_s was independent of the total thickness of Ni/Al, indicating that the measured n_s and μ were not dependent on the center metal resistivity. In addition, μ never exceeds 2000 cm^2/V s if electrons flow in the metallic layer.

Further experiments showed that μ also depended on the species of the bottom metal and had a close correlation with the thermal expansion coefficient of the bottom metal, as shown in Fig. 10, where the top metal was Al [73]. It was found that μ was more increased with a metal having larger thermal expansion coefficient and a value of over 3000 cm^2/V s was obtained with Cu/Al.

From a series of experiments, a model was proposed for the increases in n_s and μ by annealing as follows. The center metal, expanded with the temperature increase, induces a tensile strain in AlGaN/GaN layer, resulting in the increase in n_s due to the increase in piezoelectric charge. The key of this process is that the induced tensile strain brings about inelastic deformation at high temperatures and maintains it after cooling the sample to room temperature. The increase in μ is accompanied by the increase in n_s, presumably due to the reduced effective mass [66], and/or increased electron screening [74]. The larger thermal expansion coefficient of Cu and Ni induces a stronger tensile strain at high temperatures, and thus, higher μ is observed with Cu and Ni. To confirm the validity of the model, Raman microprobe spectroscopy measurements have been performed. An Ar laser with a wavelength of 496.5 nm was used as an incident beam and the Raman shift was measured on the AlGaN surface close to the Ni/Al metal (1 μm apart from the metal edge). Fig. 11 shows the measured stress for three samples, i.e., bare AlGaN surface without Ni/Al, as-deposited Ni/Al (100/100 nm), and annealed Ni/Al (100/100 nm) at 1020 K. Note that the stress value is plotted as the deviation from that for the bare surface. The increased tensile stress was 7 and 20.6 MPa for samples of as-deposited Ni/Al and annealed Ni/Al, respectively, indicating the evidence that an additional tensile stress was introduced by metal deposition and annealing.

The thermal annealing technique with a metal stack mentioned above is effective to increase both n_s and μ, and hence to reduce sheet resistance drastically. For example, the sheet resistance of AlGaN/GaN heterostructure after annealing with Ni/Al was as low as 10 Ω/sq, which is fifty times lower than that before annealing. The decreased sheet resistance will be useful to reduce the access resistance between source and gate, leading to improvement in transconductance and reduction in ON-resistance in AlGaN/GaN HEMTs.

IV. Current Collapse

It is widely known that applying high drain biases into GaN-based HEMTs frequently gives rise to the decrease in drain current accompanied by the increase in the dynamic ON-resistance. This undesirable phenomenon is known as current collapse and must be eliminated before pushing GaN-based HEMT devices into market. Since the pioneering work on the fabrication of AlGaN/GaN HEMTs [75], extensive efforts have been made to suppress current collapse and to elucidate the origin of it. It is widely recognized that current collapse can be effectively mitigated by surface passivation, especially with a SiN film [76]. The proper surface treatment before depositing surface passivation films is also reported to be effective to reduce current collapse. One such example is the surface treatment by oxygen plasma exposure. The results are shown in Fig. 12, where the dynamic ON-resistance of AlGaN/GaN HEMTs after oxygen plasma treatment with an RF power of 100 W for 60 s is dramatically reduced after passivation with either SiN, SiO_2, or AlN [77]. The oxygen termination of unbonded Ga and Al atoms near the AlGaN surface may be responsible for the reduced current collapse, and the evidence of reduced trap levels after oxygen plasma exposure has been identified by analyzing transients

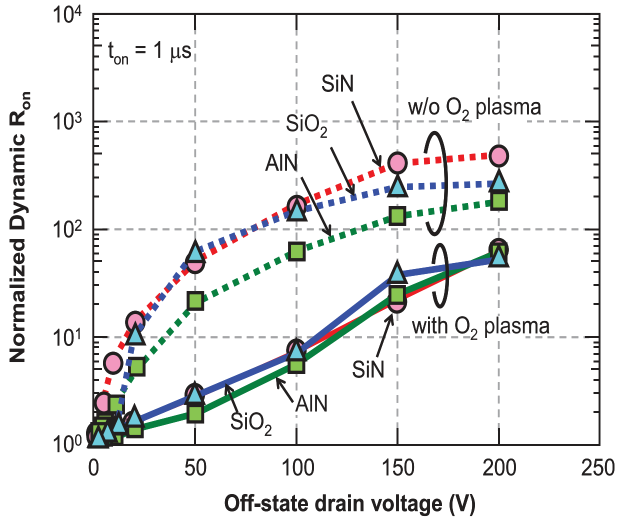

Fig. 12. Dynamic ON-resistance as a function of OFF-state drain voltage for devices with and without O_2 plasma treatment passivated with SiN, SiO_2, and AlN.

of ON-state drain current assuming Shockley-Read-Hall statistics [77].

The use of FP is another way for the suppression of current collapse. The comprehensive study on the effect of FP on the dynamic ON-resistance has been performed by preparing a series of AlGaN/GaN HEMTs with different FP lengths and gate-to-drain distance [78]. The results indicated that current collapse was dramatically improved by the introduction of gate FP, and the improvement was more enhanced using a longer FP length. It was also found that the current collapse reduction was more pronounced when the gate bias during ON-state was chosen at more positive values, suggesting that the gate FP is capable of instantly supplying additional electrons into the channel access region [78].

Although current collapse is recognized as closely related to carrier trapping phenomenon, its origin is not yet fully understood. Since current collapse was found to be affected by surface passivation, surface treatment, and the use of FP, it must be at least ascribed to trapping and detrapping of carriers at the semiconductor surface. However, several reports also suggested that the collapse was likely to be brought about from bulk traps in the buffer layer [79], [80]. Therefore, more work is definitely needed for the elimination of current collapse, including further optimization of surface processing and the reduction of bulk traps in the epitaxial layers.

V. Free-Standing GaN Substrate

AlGaN/GaN heterostructures have been commonly grown on various substrates, such as sapphire, SiC, and Si. However, a large lattice mismatch between GaN and a foreign substrate leads to generation of high density of threading dislocations on the orders of 10^8–10^{10} cm^{-2} in the epitaxial layer. Hence, the development of free-standing GaN substrates with low-dislocation densities becomes extremely important. Several groups have reported that a free-standing GaN substrate grown by hydride vapor phase epitaxy (HVPE) is effective to obtain ideal Schottky or p-n diode characteristics [81], [82].

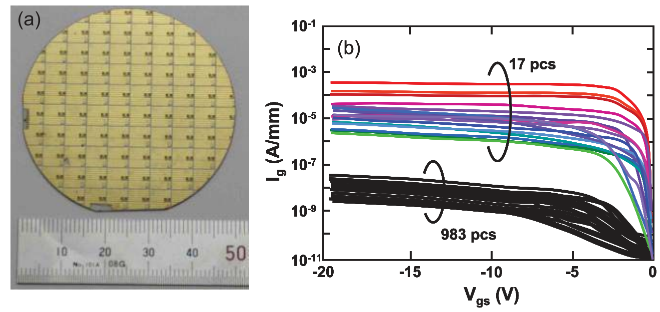

Fig. 13. (a) Top view image of AlGaN/GaN HEMTs fabricated on 2-in diameter Na-flux bulk GaN substrate. (b) Gate leakage characteristics for 1000 HEMTs.

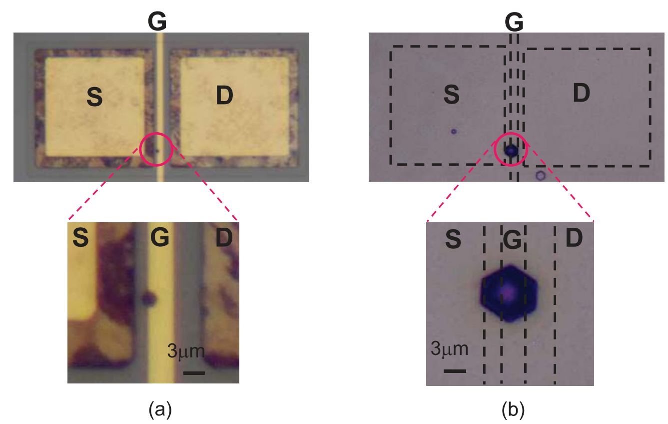

Fig. 14. Top view images of (a) device with metal electrodes and (b) device after etching off metal electrodes.

Although the dislocation density in the epitaxial layers can be significantly reduced by the use of HVPE-grown GaN substrate, the current dislocation density still stays as high as 10^6 cm^{-2}, and further reduction is required. A melt-grown method, such as Na-flux liquid phase epitaxy, has recently attracted significant attention to further reduce the dislocation density in a bulk GaN substrate [83], [84].

Using a free-standing GaN substrate with a dislocation density of less than 10^6 cm^{-2} grown by Na-flux method, our group have studied the detailed correlation between the gate leakage current in AlGaN/GaN HEMTs and point defects in the starting GaN substrate [85]. The epitaxial layers consisted of an undoped GaN channel layer and a 25-nm undoped AlGaN barrier layer with an Al composition of 0.25. Fig. 13(a) shows a top view of the whole 2-in wafer after device fabrication.

The statistical data of the reverse gate leakage current were taken from randomly selected 1000 devices fabricated on a same wafer with a gate length of 3 μm. As shown in Fig. 13(b), there observed a large scatter by more than five orders of magnitude in the reverse gate leakage characteristics measured at a gate voltage of -20 V. The leakage characteristics were divided into two groups showing low- and high-gate leakage currents, i.e., almost all the devices (983 pcs.) showed a leakage current of $< 10^{-7}$ A/mm, whereas only 17 devices exhibited rather high leakage of $>10^{-6}$ A/mm.

After electrical measurements, device areas were immersed in hot H_3PO_4 solution for 60 min to expose the surface of the GaN substrate. As shown in Fig. 14(a) and (b), there was a clear correspondence between locations of the gate electrode and the exposed hexagonal etch-pit defect with a size of several micrometers, indicating that the gate electrode of the leaky HEMT was formed in direct contact with the location of the etch-pit defect. These results suggest that the reverse gate leakage characteristics of GaN-based HEMTs are strongly influenced by the density of threading dislocations propagating through the substrate material, and thus continued efforts are of particular importance to reduce the density of point defects, and/or threading dislocations in free-standing GaN substrates.

VI. Conclusion

Technological advances for increasing the breakdown voltage, reducing the ON-resistance, suppressing current collapse, and reducing the gate leakage current in AlGaN/GaN HEMTs have been described. Comprehensive characterization on breakdown voltages in AlGaN/GaN HEMTs suggested that balancing of net positive and negative charges in the AlGaN barrier was likely to account for the experimentally observed linear dependence of breakdown voltage on the gate-to-drain distance. However, the measured lateral critical electric field was still much lower than the theoretical limit. Attempts to achieve lower contact resistances for an AlGaN-channel HEMT indicated that a new metal stack of Zr/Al/Mo/Au was effective and resulted in improved device stability at temperatures up to 300 °C. Extremely, low sheet resistance as well as high room temperature mobility exceeding 2500 $cm^2/V\,s$ were achieved for an AlGaN/GaN heterostructure deposited with a metal stack, such as Ti/Al, Ni/Al, and Cu/Al. A model was proposed in which inelastic tensile strain plays a key role. Effects of oxygen plasma treatment and providing FP were presented to reduce current collapse in AlGaN/GaN HEMTs and their mechanisms were discussed. The results strongly suggested the need for essential reduction in trapping states located on the surface or the bulk of the semiconductors. Finally, issues associated with the high-defect density in currently available AlGaN/GaN epitaxial layers are presented and the strong demand for the development of low-defect density bulk GaN substrates were pointed out.

Acknowledgment

The authors would like to thank R. Sakai, N. Yamada, R. Hasegawa, T. Asano, and Y. Kamiya for their contribution.

References

[1] D. Visalli *et al.*, "High breakdown voltage in AlGaN/GaN/AlGaN double heterostructures grown on 4 inch Si substrates," *Phys. Status Solidi C*, vol. 6, no. 2, pp. S988–S991, 2009.

[2] D. Visalli *et al.*, "AlGaN/GaN/AlGaN double heterostructures on silicon substrates for high breakdown voltage field-effect transistors with low on-resistance," *Jpn. J. Appl. Phys.*, vol. 48, no. 4S, p. 04C101, 2009.

[3] K. S. Boutros *et al.*, "Normally-off 5 A/1100 V GaN-on-silicon device for high voltage applications," in *IEEE IEDM Tech. Dig.*, Dec. 2009, pp. 161–163.

[4] K. Ota, K. Endo, Y. Okamoto, Y. Ando, H. Miyamoto, and H. Shimawaki, "A normally-off GaN FET with high threshold voltage uniformity using a novel piezo neutralization technique," in *IEEE IEDM Tech. Dig.*, Dec. 2009, pp. 153–156.

[5] B. Lu and T. Palacios, "High breakdown (>1500 V) AlGaN/GaN HEMTs by substrate-transfer technology," *IEEE Electron Device Lett.*, vol. 31, no. 9, pp. 951–953, Sep. 2010.

[6] F. Medjdoub *et al.*, "Low on-resistance high-breakdown normally off AlN/GaN/AlGaN DHFET on Si substrate," *IEEE Electron Device Lett.*, vol. 31, no. 2, pp. 111–113, Feb. 2010.

[7] T. Morita *et al.*, "99.3% efficiency of three-phase inverter for motor drive using GaN-based gate injection transistors," in *Proc. 26th Appl. Power Electron. Conf. Expo.*, Mar. 2011, pp. 481–484.

[8] H.-S. Lee, D. Piedra, M. Sun, X. Gao, S. Guo, and T. Palacios, "3000-V 4.3-$m\Omega \cdot cm^2$ InAlN/GaN MOSHEMTs with AlGaN back barrier," *IEEE Electron Device Lett.*, vol. 33, no. 7, pp. 982–984, Jul. 2012.

[9] M. Sun, H.-S. Lee, B. Lu, D. Piedra, and T. Palacios, "Comparative breakdown study of mesa- and ion-implantation-isolated AlGaN/GaN high-electron-mobility transistors on Si substrate," *Appl. Phys. Exp.*, vol. 5, no. 7, p. 074202, 2012.

[10] J.-G. Lee, B.-R. Park, H.-J. Lee, M. Lee, K.-S. Seo, and H.-Y. Cha, "State-of-the-art AlGaN/GaN-on-Si heterojunction field effect transistors with dual field plates," *Appl. Phys. Exp.*, vol. 5, no. 6, p. 066502, 2012.

[11] X. Liu *et al.*, "AlGaN/GaN-on-silicon metal–oxide–semiconductor high-electron-mobility transistor with breakdown voltage of 800 V and on-state resistance of 3 $m\Omega \cdot cm^2$ using a complementary metal–oxide–semiconductor compatible gold-free process," *Appl. Phys. Exp.*, vol. 5, no. 6, p. 066501, 2012.

[12] D. Christy *et al.*, "Uniform growth of AlGaN/GaN high electron mobility transistors on 200 mm silicon (111) substrate," *Appl. Phys. Exp.*, vol. 6, no. 2, p. 026501, 2013.

[13] Q. Jiang, C. Liu, Y. Lu, and K. J. Chen, "1.4-kV AlGaN/GaN HEMTs on a GaN-on-SOI platform," *IEEE Electron Device Lett.*, vol. 34, no. 3, pp. 357–359, Mar. 2013.

[14] T. Nanjo *et al.*, "AlGaN channel HEMT with extremely high breakdown voltage," *IEEE Trans. Electron Devices*, vol. 60, no. 3, pp. 1046–1053, Mar. 2013.

[15] X. Liu *et al.*, "AlGaN/GaN metal–oxide–semiconductor high-electron-mobility transistors with a high breakdown voltage of 1400 V and a complementary metal–oxide–semiconductor compatible gold-free process," *Jpn. J. Appl. Phys.*, vol. 52, no. 4S, p. 04CF06, Apr. 2013.

[16] B.-R. Park, J.-G. Lee, W. Choi, H. Kim, K.-S. Seo, and H.-Y. Cha, "High-quality ICPCVD SiO_2 for normally off AlGaN/GaN-on-Si recessed MOSHFETs," *IEEE Electron Device Lett.*, vol. 34, no. 3, pp. 354–356, Mar. 2013.

[17] Z. Tang, S. Huang, Q. Jiang, S. Liu, C. Liu, and K. J. Chen, "High-voltage (600-V) low-leakage low-current-collapse AlGaN/GaN HEMTs with AlN/SiN_x passivation," *IEEE Electron Device Lett.*, vol. 34, no. 3, pp. 366–368, Mar. 2013.

[18] Q. Zhou *et al.*, "Schottky-contact technology in InAlN/GaN HEMTs for breakdown voltage improvement," *IEEE Trans. Electron Devices*, vol. 60, no. 3, pp. 1075–1081, Mar. 2013.

[19] Y. Dora, A. Chakraborthy, L. McCarthy, S. Keller, S. P. DenBaars, and U. K. Mishra, "High breakdown voltage achieved on AlGaN/GaN HEMTs with integrated slant field plates," *IEEE Electron Device Lett.*, vol. 27, no. 9, pp. 713–715, Sep. 2006.

[20] Y. C. Choi, M. Pophristic, B. Peres, M. G. Spencer, and L. F. Eastman, "Fabrication and characterization of high breakdown voltage AlGaN/GaN heterojunction field effect transistors on sapphire substrates," *J. Vac. Sci. Technol. B*, vol. 24, pp. 2601–2605, Nov./Dec. 2006.

[21] N. Ikeda, K. Kato, K. Kondoh, H. Kambayashi, J. Li, and S. Yoshida, "Over 55 A, 800 V high power AlGaN/GaN HFETs for power switching application," *Phys. Status Solidi A*, vol. 204, no. 6, pp. 2028–2031, 2007.

[22] E. Bahat-Treidel, F. Brunner, O. Hilt, E. Cho, J. Würfl, and G. Tränkle, "AlGaN/GaN/GaN:C back-barrier HFETs with breakdown voltage of over 1 kV and low $R_{on} \times A$," *IEEE Trans. Electron Devices*, vol. 57, no. 11, pp. 3050–3058, Nov. 2010.

[23] P. Srivastava *et al.*, "Record breakdown voltage (2200 V) of GaN DHFETs on Si with 2-μm buffer thickness by local substrate removal," *IEEE Electron Device Lett.*, vol. 32, no. 1, pp. 30–32, Jan. 2011.

[24] M. Wang *et al.*, "900 V/1.6 $m\Omega \cdot cm^2$ normally off Al_2O_3/GaN MOSFET on silicon substrate," *IEEE Trans. Electron Devices*, vol. 61, no. 6, pp. 2035–2040, Jun. 2014.

[25] W. Choi, O. Seok, H. Ryu, H.-Y. Cha, and K.-S. Seo, “High-voltage and low-leakage-current gate recessed normally-off GaN MIS-HEMTs with dual gate insulator employing PEALD-SiN_x/RF-sputtered-HfO_2,” *IEEE Electron Device Lett.*, vol. 35, no. 2, pp. 175–177, Feb. 2014.

[26] S. Russo and A. Di Carlo, “Influence of the source–gate distance on the AlGaN/GaN HEMT performance,” *IEEE Trans. Electron Devices*, vol. 54, no. 5, pp. 1071–1075, May 2007.

[27] R. Vetury, N. Q. Zhang, S. Keller, and U. K. Mishra, “The impact of surface states on the DC and RF characteristics of AlGaN/GaN HFETs,” *IEEE Trans. Electron Devices*, vol. 48, no. 3, pp. 560–566, Mar. 2001.

[28] N. Tipirneni, A. Koudymov, V. Adivarahan, J. Yang, G. Simin, and M. A. Khan, “The 1.6-kV AlGaN/GaN HFETs,” *IEEE Electron Device Lett.*, vol. 27, no. 9, pp. 716–718, Sep. 2006.

[29] J. P. Ibbetson, P. T. Fini, K. D. Ness, S. P. DenBaars, J. S. Speck, and U. K. Mishra, “Polarization effects, surface states, and the source of electrons in AlGaN/GaN heterostructure field effect transistors,” *Appl. Phys. Lett.*, vol. 77, no. 2, pp. 250–252, Jul. 2000.

[30] S. G. Nassif-Khalil and C. A. T. Salama, “Super-junction LDMOST on a silicon-on-sapphire substrate,” *IEEE Trans. Electron Devices*, vol. 50, no. 5, pp. 1385–1391, May 2003.

[31] H. Ishida *et al.*, “Unlimited high breakdown voltage by natural super junction of polarized semiconductor,” *IEEE Electron Device Lett.*, vol. 29, no. 10, pp. 1087–1089, Oct. 2008.

[32] Y. Ando, Y. Okamoto, H. Miyamoto, T. Nakayama, and M. Kuzuhara, “10-W/mm AlGaN-GaN HFET with a field modulating plate,” *IEEE Electron Device Lett.*, vol. 24, no. 5, pp. 289–291, May 2003.

[33] Y.-F. Wu *et al.*, “30-W/mm GaN HEMTs by field plate optimization,” *IEEE Electron Device Lett.*, vol. 25, no. 3, pp. 117–119, Mar. 2004.

[34] Y. Okamoto *et al.*, “Improved power performance for a recessed-gate AlGaN-GaN heterojunction FET with a field-modulating plate,” *IEEE Trans. Microw. Theory Techn.*, vol. 52, no. 11, pp. 2536–2540, Nov. 2004.

[35] H. Xing, Y. Dora, A. Chini, S. Heikman, S. Keller, and U. K. Mishra, “High breakdown voltage AlGaN-GaN HEMTs achieved by multiple field plates,” *IEEE Electron Device Lett.*, vol. 25, no. 4, pp. 161–163, Apr. 2004.

[36] Y. Ando *et al.*, “Novel AlGaN/GaN dual-field-plate FET with high gain, increased linearity and stability,” in *IEEE IEDM Tech. Dig.*, Dec. 2005, pp. 585–588.

[37] T. Deguchi *et al.*, “Suppression of current collapse of high-voltage AlGaN/GaN HFETs on Si substrates by utilizing a graded field-plate structure,” in *Proc. TWHM*, 2011, pp. 67–68.

[38] M. A. Khan *et al.*, “AlGaN/GaN metal oxide semiconductor heterostructure field effect transistor,” *IEEE Electron Device Lett.*, vol. 21, no. 2, pp. 63–65, Feb. 2000.

[39] M. Ochiai, M. Akita, Y. Ohno, S. Kishimoto, K. Maezawa, and T. Mizutani, “AlGaN/GaN heterostructure metal-insulator-semiconductor high-electron-mobility transistors with Si_3N_4 Gate Insulator,” *Jpn. J. Appl. Phys.*, vol. 42, no. 4B, pp. 2278–2280, Apr. 2003.

[40] Z. H. Liu, G. I. Ng, S. Arulkumaran, Y. K. T. Maung, and H. Zhou, “Temperature-dependent forward gate current transport in atomic-layer-deposited Al2O3/AlGaN/GaN metal-insulator-semiconductor high electron mobility transistor,” *Appl. Phys. Lett.*, vol. 98, no. 16, p. 163501, Apr. 2011.

[41] S. Rai *et al.*, “Low threshold-14 W/mm ZrO_2/AlGaN/GaN metal–oxide–semiconductor heterostructure field effect transistors,” *Jpn. J. Appl. Phys.*, vol. 45, no. 6A, pp. 4985–4987, Jun. 2006.

[42] J. Shi and L. F. Eastman, “Correlation between AlGaN/GaN MISHFET performance and HfO_2 insulation layer quality,” *IEEE Electron Device Lett.*, vol. 32, no. 3, pp. 312–314, Mar. 2011.

[43] C. Y. Chang *et al.*, “Development of enhancement mode AlN/GaN high electron mobility transistors,” *Appl. Phys. Lett.*, vol. 94, no. 26, p. 263505, Jun. 2009.

[44] M. Higashiwaki *et al.*, “A comparative study of effects of SiN_x deposition method on AlGaN/GaN heterostructure field-effect transistors,” *Appl. Phys. Lett.*, vol. 94, no. 5, p. 053513, Feb. 2009.

[45] Z. H. Liu *et al.*, “High microwave-noise performance of AlGaN/GaN MISHEMTs on silicon with Al_2O_3 gate insulator grown by ALD,” *IEEE Electron Device Lett.*, vol. 31, no. 2, pp. 96–98, Feb. 2010.

[46] K.-T. Lee, C.-F. Huang, J. Gong, and C.-T. Lee, “ High performance 1 μm GaN n- MOSFET with MgO/MgO-TiO_2 stacked gate dielectrics,” *IEEE Electron Device Lett.*, vol. 32, no. 3, pp. 306–308, Mar. 2011.

[47] F. Ren *et al.*, “Effect of temperature on $Ga_2O_3(Gd_2O_3)$/GaN metal–oxide–semiconductor field-effect transistors,” *Appl. Phys. Lett.*, vol. 73, no. 26, pp. 3893–3895, Dec. 1998.

[48] S. Dasgupta *et al.*, “Self-aligned technology for N-polar GaN/Al(Ga)N MIS-HEMTs,” *IEEE Electron Device Lett.*, vol. 32, no. 1, pp. 33–35, Jan. 2011.

[49] M. Hatano, Y. Taniguchi, S. Kodama, H. Tokuda, and M. Kuzuhara, “Reduced gate leakage and high thermal stability of AlGaN/GaN MIS-HEMTs using ZrO_2/Al_2O_3 gate dielectric stack,” *Appl. Phys. Exp.*, vol. 7, no. 4, p. 044101, 2014.

[50] A. N. Bright, P. J. Thomas, M. Weyland, D. M. Tricker, C. J. Humphreys, and R. Davies, “Correlation of contact resistance with microstructure for Au/Ni/Al/Ti/AlGaN/GaN ohmic contacts using transmission electron microscopy,” *J. Apply. Phys.*, vol. 89, no. 6, pp. 3143–3150, Mar. 2001.

[51] D. Qiao, L. S. Yu, L. Jia, P. M. Asbeck, S. S. Lau, and T. E. Haynes, “Transport properties of the advancing interface ohmic contact to AlGaN/GaN heterostructures,” *Appl. Phys. Lett.*, vol. 80, no. 6, pp. 992–994, Feb. 2002.

[52] T. Nakayama *et al.*, “Low-contact-resistance and smooth-surface Ti/Al/Nb/Au ohmic electrode on AlGaN/GaN heterostructure,” *Appl. Phys. Lett.*, vol. 85, no. 17, pp. 3775–3776, Oct. 2004.

[53] F. M. Mohammed, L. Wang, and I. Adesida, “Noninterfacial-nitride formation ohmic contact mechanism in Si-containing Ti/Al/Mo/Au metallizations on AlGaN/GaN heterostructures,” *Appl. Phys. Lett.*, vol. 87, no. 26, p. 262111, Dec. 2005.

[54] A. Vertiatchikh, E. Kaminsky, J. Teetsov, and K. Robinson, “Structural properties of alloyed Ti/Al/Ti/Au and Ti/Al/Mo/Au ohmic contacts to AlGaN/GaN,” *Solid-State Electron.*, vol. 50, nos. 7–8, pp. 1425–1429, 2006.

[55] H.-S. Lee, D. S. Lee, and T. Palacios, “AlGaN/GaN high-electron-mobility transistors fabricated through a Au-free technology,” *IEEE Electron Device Lett.*, vol. 32, no. 5, pp. 623–625, May 2011.

[56] M. Van Hove *et al.*, “CMOS process-compatible high-power low-leakage AlGaN/GaN MISHEMT on silicon,” *IEEE Electron Device Lett.*, vol. 33, no. 5, pp. 667–669, May 2012.

[57] N. Yafune, S. Hashimoto, K. Akita, Y. Yamamoto, and M. Kuzuhara, “Low-resistive ohmic contacts for AlGaN channel high-electron-mobility transistors using Zr/Al/Mo/Au metal stack,” *Jpn. J. Appl. Phys.*, vol. 50, no. 10R, p. 100202, Oct. 2011.

[58] H. Tokuda *et al.* “High Al composition AlGaN-channel high-electron-mobility transistor on AlN substrate,” *Appl. Phys. Exp.*, vol. 3, no. 12, p. 121003, Dec. 2010.

[59] M. Hatano *et al.*, “Superior DC and RF performance of AlGaN-channel HEMT at high temperatures,” *IEICE Trans. Electron.*, vol. E95-C, no. 8, pp. 1332–1336, Aug. 2012.

[60] J. M. Redwing *et al.*, “Two-dimensional electron gas properties of AlGaN/GaN heterostructures grown on 6H-SiC and sapphire substrates,” *Appl. Phys. Lett.*, vol. 69, no. 7, pp. 963–965, Aug. 1996.

[61] M. J. Manfra, K. W. Baldwin, A. M. Sergent, K. W. West, R. J. Molnar, and J. Caissie, “Electron mobility exceeding 160000 cm^2/Vs in AlGaN/GaN heterostructures grown by molecular-beam epitaxy,” *Appl. Phys. Lett.*, vol. 85, no. 22, pp. 5394–5396, Nov. 2004.

[62] L. Hsu and W. Walukiewicz, “Electron mobility in $Al_xGa_{1-x}N$/GaN heterostructures,” *Phys. Rev. B*, vol. 56, no. 3, pp. 1520–1528, Jul. 1997.

[63] I. P. Smorchkova *et al.*, “Polarization-induced charge and electron mobility in AlGaN/GaN heterostructures grown by plasma-assisted molecular-beam epitaxy,” *J. Appl. Phys.*, vol. 86, no. 8, pp. 4520–4526, Oct. 1999.

[64] R. Gaska *et al.*, “Electron transport in AlGaN–GaN heterostructures grown on 6H-SiC substrates,” *Appl. Phys. Lett.*, vol. 72, no. 6, pp. 707–709, Feb. 1998.

[65] J. W. Chung, W. E. Hoke, E. M. Chumbes, and T. Palacios, “AlGaN/GaN HEMT with 300-GHz f_{max},” *IEEE Electron Device Lett.*, vol. 31, no. 3, pp. 195–197, Mar. 2010.

[66] M. Azize and T. Palacios, “Effect of substrate-induced strain in the transport properties of AlGaN/GaN heterostructures,” *J. Appl. Phys.*, vol. 108, no. 2, pp. 023707-1–023707-4, Jul. 2010.

[67] T. B. Fehlberg *et al.*, “Transport studies of AlGaN/GaN heterostructures of different Al mole fractions with variable SiN_x passivation stress,” *IEEE Trans. Electron Devices*, vol. 58, no. 8, pp. 2589–2596, Aug. 2011.

[68] K.-S. Im *et al.*, “Normally off GaN MOSFET based on AlGaN/GaN heterostructure with extremely high 2DEG density grown on silicon substrate,” *IEEE Electron Device Lett.*, vol. 31, no. 3, pp. 192–194, Mar. 2010.

[69] H. Tokuda, T. Kojima, and M. Kuzuhara, “A method to increase sheet electron density and mobility by vacuum annealing for Ti/Al deposited AlGaN/GaN heterostructures,” *Appl. Phys. Lett.*, vol. 101, no. 8, pp. 082111-1–082111-4, Aug. 2012.

[70] H. Tokuda, T. Kojima, and M. Kuzuhara, “Role of Al and Ti for ohmic contact formation in AlGaN/GaN heterostructures,” *Appl. Phys. Lett.*, vol. 101, no. 26, p. 262104, 2012.
[71] T. Kojima, H. Tokuda, and M. Kuzuhara, “Comparison of 2DEG density and mobility increase by annealing AlGaN/GaN heterostructures deposited with Ti/Al, Ti/Au, V/Au, and Ni/Au,” *Phys. Status Solidi C*, vol. 10, no. 11, pp. 1405–1408, Nov. 2013.
[72] H. Tokuda, T. Kojima, and M. Kuzuhara, “Over 3000 cm^2 V^{-1} s^{-1} room temperature two-dimensional electron gas mobility by annealing Ni/Al deposited on AlGaN/GaN heterostructures,” *Appl. Phys. Exp.*, vol. 7, no. 4, p. 041001, 2014.
[73] G. Kawaguchi, T. Kojima, H. Tokuda, and M. Kuzuhara, “Enhanced 2DEG mobility by thermally induced strain between deposited metals and AlGaN/GaN heterostructures,” presented at the ISCS, Montpellier, France, May 2014.
[74] X. Z. Dang *et al.*, “Measurement of drift mobility in AlGaN/GaN heterostructure field-effect transistor,” *Appl. Phys. Lett.*, vol. 74, no. 25, pp. 3890–3892, Jun. 1999.
[75] M. A. Khan, A. Bhattarai, J. N. Kuznia, and D. T. Olson, “High electron mobility transistor based on a GaN-$Al_xGa_{1-x}N$ heterojunction,” *Appl. Phys. Lett.*, vol. 63, no. 9, pp. 1214–1215, Aug. 1993.
[76] H. Kim, R. M. Thompson, V. Tilak, T. R. Prunty, J. R. Shealy, and L. F. Eastman, “Effects of SiN passivation and high-electric field on AlGaN-GaN HFET degradation,” *IEEE Electron Device Lett.*, vol. 24, no. 7, pp. 421–423, Jul. 2003.
[77] Y. Sakaida, H. Tokuda, and M. Kuzuhara, “Improved current collapse in AlGaN/GaN HEMTs by O_2 plasma treatment,” in *Dig. CSMANTECH*, Denver, CO, USA, 2014, pp. 197–200.
[78] M. T. Hasan, T. Asano, H. Tokuda, and M. Kuzuhara, “Current collapse suppression by gate field-plate in AlGaN/GaN HEMTs,” *IEEE Electron Device Lett.*, vol. 34, no. 11, pp. 1379–1381, Nov. 2013.
[79] M. Faqir *et al.*, “Mechanisms of RF current collapse in AlGaN–GaN high electron mobility transistors,” *IEEE Trans. Device Mater. Rel.*, vol. 8, no. 2, pp. 240–247, Jun. 2008.
[80] D. Bisi *et al.*, “Deep-level characterization in GaN HEMTs—Part I: Advantages and limitations of drain current transient measurements,” *IEEE Trans. Electron Devices*, vol. 60, no. 10, pp. 3166–3175, Oct. 2013.
[81] J. Suda *et al.*, “Nearly ideal current–voltage characteristics of Schottky barrier diodes formed on hydride-vapor-phase-epitaxy-grown GaN free-standing substrates,” *Appl. Phys. Exp.*, vol. 3, no. 10, p. 101003, 2010.
[82] I. C. Kizilyalli, A. P. Edwards, H. Nie, D. Disney, and D. Bour, “High voltage vertical GaN p-n diodes with avalanche capability,” *IEEE Trans. Electron Devices*, vol. 60, no. 10, pp. 3067–3070, Oct. 2013.
[83] F. Kawamura *et al.*, “Drastic decrease in dislocations during liquid phase epitaxy growth of GaN single crystals using Na flux method without any artificial processes,” *Jpn. J. Appl. Phys.*, vol. 45, no. 4A, pp. 2528–2530, 2006.
[84] M. Imade *et al.*, “Growth of large GaN single crystals on high-quality GaN seed by carbon-added Na flux method,” *Appl. Phys. Exp.*, vol. 3, no. 7, p. 075501, Jul. 2010.
[85] R. Hasegawa, N. Yafune, H. Tokuda, Y. Mori, H. Amano, and M. Kuzuhara, “Effects of substarte defects on the gate leakage current of AlGaN/GaN heterojunction FETs on Na flux bulk GaN,” in *Proc. Extended Abstracts Int. Conf. Solid State Devices Mater.*, Nagoya, Japan, 2011, pp. 620–621.

Masaaki Kuzuhara (M’82–SM’01–F’05) was born in Osaka, Japan, in 1955. He received the B.S., M.S., and Ph.D. degrees in electrical engineering from Kyoto University, Kyoto, Japan, in 1979, 1981, and 1991, respectively.

He is currently a Professor with the Department of Electrical and Electronics Engineering, University of Fukui, Fukui, Japan, where he is focusing on III-N device physics and characterization.

Hirokuni Tokuda received the Ph.D. degree in electronics engineering from the University of Tokyo, Tokyo, Japan, in 1978.

He joined Murata Manufacturing Company, Ltd., Kyoto, Japan, in 2002, where he was the General Manager of the Department of Antenna Products. Since 2009, he has been with the University of Fukui, Fukui, Japan. His research interests include GaN-based HEMT devices and their physics.